



ELSEVIER

Contents lists available at ScienceDirect

## Optics Communications

journal homepage: [www.elsevier.com/locate/optcom](http://www.elsevier.com/locate/optcom)

# Calculation method of the overlap factor and its enhancement for airborne lidar



Ruiqiang Chen, Yuesong Jiang\*, Haiyang Wang

Department of Electronic &amp; Information Engineering, Beihang University, Beijing 100191, China

## ARTICLE INFO

## Article history:

Received 6 January 2014  
 Received in revised form  
 29 May 2014  
 Accepted 30 May 2014  
 Available online 12 June 2014

## Keywords:

Airborne lidar  
 Overlap factor  
 Laser intensity distribution  
 Ray-tracing method  
 Field lens

## ABSTRACT

We present an airborne lidar overlap factor calculation method based on laser intensity distribution and ray-tracing method. It is a comparatively simpler solution than analytical-based methods, and can be applied to any special laser intensity distribution. In this paper, we emphatically analyze the relationship among lidar overlap factor, flight speed and scanning mirror rotating speed. The parametric simulation results of our airborne lidar indicate that the lidar overlap factor is sensitive to the scanning mirror rotating speed but insensitive to the flight speed. The overlap factor is enhanced by inserting a field lens in the focal plane of telescope, and then optimal geometry parameters of the field lens are discussed. The final simulation results prove that this enhancement approach is elegant and effective.

© 2014 Elsevier B.V. All rights reserved.

## 1. Introduction

The lidar, combined with modern laser technology and photo-electric processing technology, is an advanced remote sensing apparatus. Due to high ranging resolution, it is widely applied in many fields, such as atmospheric physics, earth resource survey, geomatics, urban planning, etc. [1–4]. Because it is an active remote measuring method by illuminating target surface and then analyzing reflected light, the overlap factor (OVF) is an effect of reduced detector response to the reflected light and is uniquely determined by lidar optical system configuration. Because of defocusing effects in the near range, the OVF is often incomplete as occurs in coaxial systems as well as in biaxial ones. Therefore, the OVF becomes a key parameter in evaluating whether or not the lidar optical system configuration satisfies specified design requirements.

There are many calculation methods for the OVF, which can be typically divided into two major groups: first the OVF based on target plane [5–8] and second the OVF based on image plane [9–14]. For the OVF based on the target plane, it is computed as the ratio between the power reaching the illustrated target plane cross-section (i.e., the circle defined by the divergence of emitted laser in the target plane) and the power collected by the telescope field of view (FOV) circle in the target plane. In general, it is simple and easily implemented but is not suitable for precisely analyzing how optical components in the optical system affect the OVF. For example, it is hard to consider obstruction

effect and defocusing effect in the image plane caused by the near-ranging illuminated target. Hence, the OVF based on the image plane is proposed for development and application of the lidar. It is computed as the ratio between the power reaching the detector active area scattered from a given range and the power collected by the receiving optics from that range. And then a ray-tracing method based on ray transfer matrix analysis (also known as ABCD matrix analysis) is used to model atmospheric propagation and optical receiving system. Theoretically, the ray-tracing method can be applied to lidar system with any special laser intensity distribution. Thus the OVF based on the image plane is more accurate but complex than the OVF based on the target plane.

According to whether or not the directions of lidar optical transmitting and receiving are both continually changing, lidar can be generally classified into two categories: first static lidar and second dynamic lidar. Researches about lidar OVF are mainly concentrated in static lidar [14,15]. Example for a ground-based atmospheric or tropospheric lidar, backscattered light signal is analyzed to retrieve information on properties of the atmosphere or troposphere along a fixed light-path during a long period (e.g., dozens of minutes). By contrast, for dynamic lidar [3,4], in order to acquire 3D information of the interested target, it has to continually change the directions of transmitting and receiving by using optical mechanical scanning apparatus. Obviously, the research of the dynamic lidar OVF will be more difficult than the static lidar OVF.

In light of that, we present an OVF calculation method for airborne lidar (i.e., typical dynamic lidar). The main goal of this method is to, first discretize laser footprint as pixel spots assembly, then calculate each pixel OVF by using ray-tracing method, finally

\* Corresponding author. Tel.: +86 13911842708.  
 E-mail address: [yuesongjiang@buaa.edu.cn](mailto:yuesongjiang@buaa.edu.cn) (Y. Jiang).

obtain the lidar OVF according to each pixel energy percentage. Case study for a typical airborne lidar is carried out that the lidar cannot work well, and the simulation results indicate the lidar OVF is sensitive to scanning mirror but insensitive to flight speed. Insertion of a field lens in the telescope focal plane is adopted to enhance the lidar OVF, and the following simulation results confirm that it is a very effective approach.

## 2. Fundamentals for airborne lidar OVF calculation

Limited to volume and weight requirements for airborne equipment, coaxial system is widely adopted in the airborne lidar. As shown in Fig. 1, it is based on Cassegrain telescope with advantages of relatively large receiving aperture and compact appearance. In emission, by means of reflector M2 and M3, emitted laser is reflected to propagate along the optical axis, and then to center of scanning mirror M1. Additionally, the scanning mirror is elliptical, and is placed at an angle of 45° with the optical axis so that its projection along the optical axis just covers the telescope aperture (i.e., the primary mirror M4) and at the same time the direction of beam transmission is perpendicular to the optical axis. In reception, part of the target backscattered light is collected by Cassegrain telescope consisted of primary parabolic mirror M4 and secondary hyperbolic mirror M5, and then focused on the detector active area which is usually placed at the focus point of the telescope for optimum collection efficiency of long-distance ray.

### 2.1. Intensity distribution model for laser footprint

First, we set up a rectangular coordinate system based on the airborne lidar optical transmitter–receiver system (Figs. 1 and 2). Where is they – axis coincides with the optical axis; z – axis along the direction of gravity; and origin point o is on the center of scanning mirror.

As shown in Fig. 2, the initial laser radius was assumed small enough so that the emitted laser beam can be considered as a cone. Because the emitted laser beam illustrates slantly on the target surface, and then the laser footprint is elliptical. For the laser footprint its center coordinate is  $(x_0, y_0, h)$ ,  $a_x$  and  $b_y$  were respectively the semi-major and semi-minor axis:

$$\begin{cases} x_0 = \frac{1}{2}h [\tan(\beta + \frac{\alpha}{2}) + \tan(\beta - \frac{\alpha}{2})] \\ y_0 = 0 \\ a_x = \frac{1}{2}h [\tan(\beta + \frac{\alpha}{2}) - \tan(\beta - \frac{\alpha}{2})] \\ b_y = h \frac{\sin(\frac{\alpha}{2})}{\sqrt{\cos(\beta - \frac{\alpha}{2})\cos(\beta + \frac{\alpha}{2})}} \end{cases} \approx \begin{cases} x_0 = h \tan(\beta) \\ y_0 = 0 \\ a_x = \frac{1}{2}h\alpha \sec^2(\beta) \\ b_y = \frac{1}{2}h\alpha \sec(\beta) \end{cases} \quad (1)$$

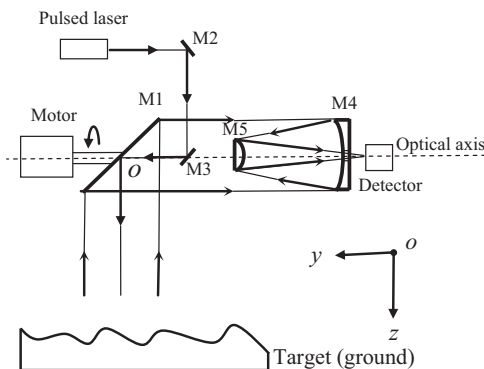


Fig. 1. Schematic diagram of coaxial transmitter–receiver system based on Cassegrain telescope.

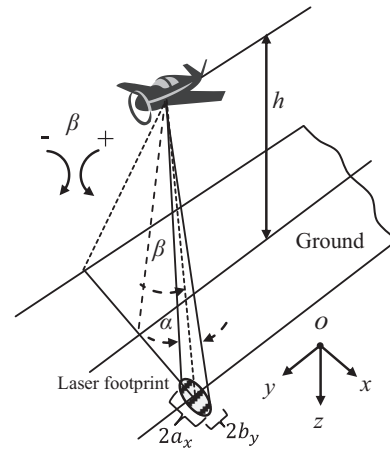


Fig. 2. Schematic diagram of laser footprint on the target surface.

Table 1  
Simulation parameters for the airborne lidar presented.

| Emitted laser                     |                      |
|-----------------------------------|----------------------|
| Mode                              | TEM <sub>00</sub>    |
| Wavelength                        | 1064 nm              |
| Divergence angle, $\alpha$        | 0.8 mrad             |
| Dimensionless parameter, $\sigma$ | 0.35                 |
| Laser receiver                    |                      |
| Type                              | Cassegrain telescope |
| Primary mirror radius, $r_T$      | 80 mm                |
| Secondary mirror radius, $r_S$    | 25 mm                |
| Focal length, $f_T$               | 666.7 mm             |
| Detector                          |                      |
| Radius, $r_D$                     | 0.4 mm               |
| Position                          | Telescope focus      |
| Scanning mirror                   |                      |
| Tilting angle, $\beta$            | –22.5° to 22.5°      |
| Rotating speed, RPS               | 40 r/s               |
| Plane                             |                      |
| Flight altitude, $h$              | ≤ 1000 m             |
| Flight speed, $v$                 | ≤ 200 km/h           |

where  $h$  is flight altitude,  $\alpha$  is the emitted laser divergence angle (full angle),  $\beta$  is the emitted laser beam cone-axis-to-oz tilting angle (positive angles counter clock wise). Because  $\alpha$  and  $\beta$  are both small enough ( $\alpha = 0.8$  mrad,  $|\beta| \leq 22.5^\circ$  in Table 1) so that we can get  $\sin(\alpha) \approx \alpha$  and  $\cos(\beta \pm (\alpha/2)) \approx \cos(\beta)$ . In this case, the left-hand side equation could yield approximately to the right-hand side equation in Eq. (1).

By using the approximate footprint ellipse parameters, it can be seen that the center of the elliptical footprint is on the laser beam cone axis, and the cross-section of the footprint can be considered as a bi-dimensional source of rays following a Gaussian intensity distribution (under the assumption that the target reflectivity is uniform):

$$p_{FP}(x, y, h) = \frac{1}{2\pi(\sigma a_x)(\sigma b_y)} e^{-\frac{1}{2} \left( \frac{(x-x_0)^2}{(\sigma a_x)^2} + \frac{(y-y_0)^2}{(\sigma b_y)^2} \right)}, \quad \frac{(x-x_0)^2}{a_x^2} + \frac{(y-y_0)^2}{b_y^2} \leq 1 \quad (2)$$

where  $p_{FP}(x, y, h)$  represents the energy percent of rays reflected by a point  $(x, y, h)$  in the laser footprint,  $\sigma$  is a dimensionless parameter,  $\sigma a_x$  and  $\sigma b_y$  represent the standard deviation of random variables  $x$  and  $y$  respectively.

As demonstrated in Fig. 3, the minimum enclosing rectangle of laser footprint is defined as  $m$  pixel by  $w(m)$  pixel square spot [7]. Then we define  $step_x$  as the side length of pixels, where it can be

Download English Version:

<https://daneshyari.com/en/article/1534465>

Download Persian Version:

<https://daneshyari.com/article/1534465>

[Daneshyari.com](https://daneshyari.com)